# Lubrication Effect of Liquid Nitrogen in Cryogenic Machining Friction on the Tool-chip Interface

**Seong-Chan Jun**
*Department of Mechanical Engineering, Columbia University, New York, NY 10027, USA*

The liquid nitrogen as an environmentally safe coolant has been widely recognized in cryogenic machining, its function as a lubricant is plausible due to its chemical inertness, physical volatility and low viscosity. Since a reduced friction is a direct witness of the lubrication effect from a tribological viewpoint, this paper presents an evaluation of the apparent friction coefficient on the tool-chip interface in cryogenic cutting operations to prove and characterize the lubricity of LN2 in cryogenic machining. The cryogenic cutting technology used in this study is based on a cooling approach and liquid nitrogen delivery system which are intended to apply liquid nitrogen in well-controlled fine jets to selectively localized cutting zones and to penetrate liquid nitrogen to the tool-chip interface. It has been found that the apparent friction coefficient can be significantly reduced in cryogenic machining, depending on the approach of liquid nitrogen delivery.

**Key Words :** Tool Wear, Tool Life, Cryogenic Machining

## 1. Introduction

Conventionally various cutting fluids have been used in cutting operations to sustain a proper machinability for most metal materials. A conventional cutting fluid, such as an emulsion, can be expected to improve tool life by reducing the temperature rise in the cutting area to maintain the tool toughness and by providing a lubrication effect to reduce the friction of the chip and work on the tool faces. This suggests that a conventional cutting fluid can serve as both a coolant and a lubricant in cutting operations. Liquid nitrogen (LN2) as an environmentally safe coolant has been widely recognized in cryogenic machining while its function as a lubricant is plausible due to its chemical inertness, physical volatility and low viscosity. Therefore, the tool life improvement in cryogenic machining, as reported widely in other researches, have been mainly attributed to the super-cooling effect of LN2 in a belief that almost all types of tool wear mechanism are governed by the tool-chip interface temperature and can be considerably reduced if the LN2 is properly applied to the cutting area.

Current cutting technology annually requires 300 million gallons of potentially polluting cutting fluids. If substitute for this, we can expect to totally prevent production of cutting fluid and avoid the environmental problems associated with internal recycle, disposal and cleanup. No new contaminants are created by the cryogenic machining process which might offset the waste savings.

In economical point of view the emulsion cooling method has more costs for not only coolant itself, in addition wasting costs and environmentally harmful to our surroundings. Each part costs $0.336 for conventional emulsion and $0.209 for 2 nozzle on in LN2 for only consumed

* **E-mail** : scj10@columbia.deu
Department of Mechanical Engineering, Columbia University, New York, NY 10027, USA. (Manuscript **Received** May 27, 2004; **Revised** October 13, 2004)

**Table 1** Tool life for cryogenic machining

| | Cutting Speed (ft/min) (m/s) | | | | Coolant Flow |
|---|---|---|---|---|---|
| | 200 (1.016) | 300 (1.524) | 400 (2.032) | 500 (2.54) | |
| Conventional Emulsion | 17 m 30s | 4 m 50s | 2 m 38s | 56s | Emulsion flood |
| 2 Nozzle LN2 | 27 m 33s | 15 m 48s | 7 m 17s | 4 m 56s | 0.215 GPM (0.8138 LPM) |

**Table 2** Productivity analysis for cryogenic machining

| | Feed Rate | Cutting Speed | Tool Life | Hourly Yield | Coolant Cost | Cost per Part |
|---|---|---|---|---|---|---|
| Conventional Emulsion | .01 inches (2.54 mm) | 300 ft/min (1.524 m/s) | 4 m 50s | 9.908 parts | $0.336/part | $7.171 |
| 2 Nozzle LN2 | .01 inches (2.54 mm) | 300 ft/min (1.524 m/s) | 15 m 48s | 12.906 parts | $0.209/part | $4.849 |
| Conventional Emulsion | .01 inches (2.54 mm) | 500 ft/min (2.54 mm/s) | 56s | 6.468 parts | $0.513/part | $13.363 |
| 2 Nozzle LN2 | .01 inches (2.54 mm) | 500 ft/min (2.54 mm/s) | 4 m 56s | 15.924 parts | $0.126/part | $4.348 |

materials, and more details described in Tables 1 and 2. In the quality matters the expected finished surface is fully accomplished and the finer surface can be obtained in LN2 cooling.

It is true that no lubrication effect can be expected of LN2 in the tool-chip interface if LN2 is delivered to a spot away from the tool-chip contact area or applied to flood indiscriminately the general cutting area as a whole. In order to generate an effective lubrication, the localized tool-chip contact area should be soaked with or directly exposed to LN2 hydraulics. Yet due to a typically high normal load on the tool face, a penetration of LN2 into the tool-chip interface is impracticable without a proper LN2 delivery approach. Such an approach should facilitate the direct exposure of the tool-chip contact area to the LN2 flow.

Hong developed a patented LN2 spraying nozzle for turning operation, which is built into the obstruction-type chip breaker and is capable of applying high pressure LN2 in a well-controlled jet to the localized tool-chip interface, instead of flooding the general cutting area. The nozzle built into the chip breaker, shown in Figures 1 and 2 leads a LN2 flow of good liquid quality

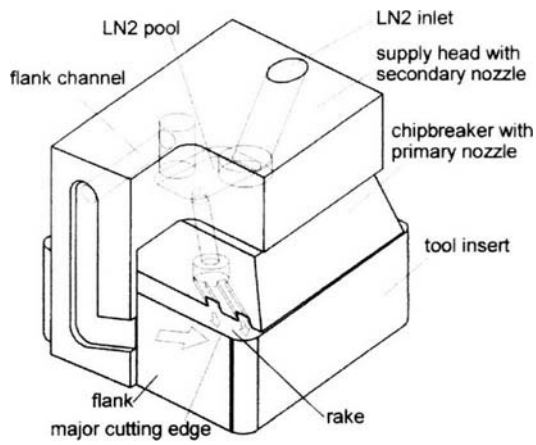


**Fig. 1** Assembly of two nozzle LN2 delivery system

to the tool-chip contact area extremely adjacent to the cutting edge. Actual liquid nitrogen injection in tool nozzle assembly is shown in Figure 3. With a high pressure for LN2 delivery and a lifting-up action of the chip breaker, LN2 can be trapped inside the space enclosed by the chip face, tool rake and obstructing face of the chip breaker and penetrate to the tool-chip interface well. Although a significant improvement in tool life has been observed in cryogenic tests based on this

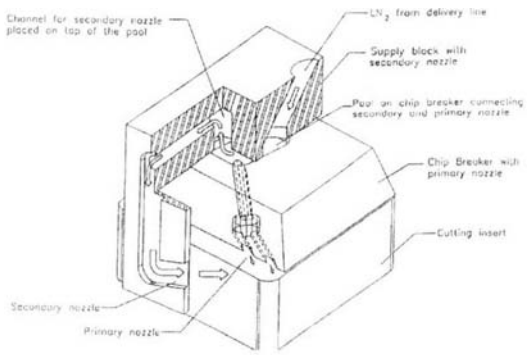


(a) When primary and auxiliary nozzle are used to inject liquid nitrogen

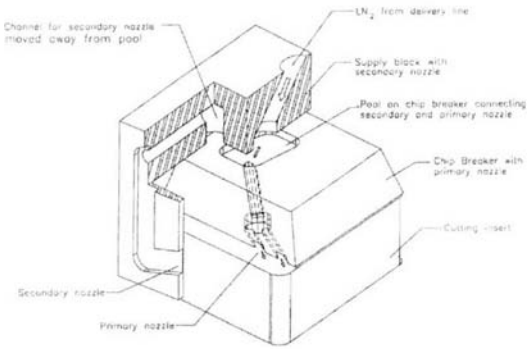


(b) Only primary nozzle is used

**Fig. 2** The design implementation of the cryogenic nozzle

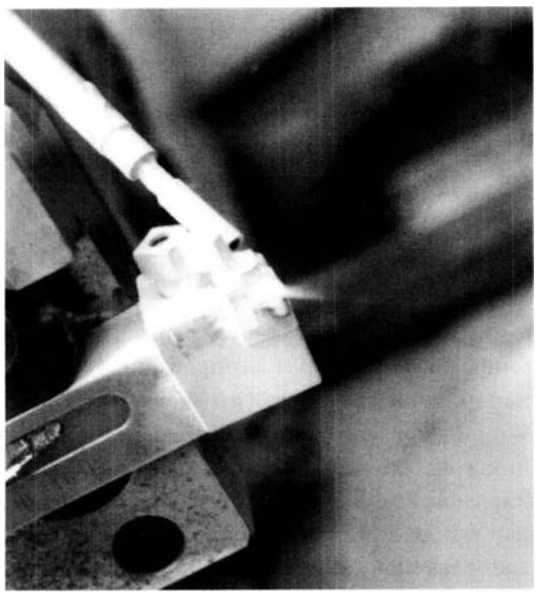

**Fig. 3** A photo of the nozzle tool assembly showing liquid nitrogen flowing

LN2 delivery approach, it would be still arbitrary to associate the reduced tool wear rate directly with the effectiveness of the intended LN2 lubrication because this LN2 delivery approach also maximizes the cooling effect of the tool.

From a tribological viewpoint, a reduced friction is a direct witness of the lubrication effect on a pair of interacting surfaces. This fact suggests that the friction on the tool-chip interface can better characterize the function of LN2 as a lubricant in a cryogenic cutting operation. Yet the friction on the tool-chip interface cannot be measured readily because of a complicated engagement of the tool with the workpiece material that is typical for a real-life industrial cutting process. Therefore, a mechanical model has to be formulated to derive the friction on the tool-chip interface from those cutting force components measured by an assembly of the toolholder and dynamometer.

This paper presents an evaluation of the apparent friction coefficient on the tool-chip interface in cryogenic cutting operations to prove and characterize the lubricity of LN2 in cryogenic machining. Three mathematical methods have been formulated to derive the apparent friction coefficient on the tool-chip interface for the industry-typical oblique cuttings based on the cutting force components measured in the directions of cutting, feeding and trusting. The cutting tests are performed for Ti-6Al-4V, a titanium alloy, AISI1018, and a low carbon steel, on a CNC turning center, and a three dimensional dynamometer has been mounted between the tool turret and tool holder to measure the cutting force components.

## 2. Models for Evaluating the Normal and Frictional Forces

In a cutting operation, the engagement of the tool with the workpiece is concentrated in two areas, namely, the tool-chip interface where the chip is pressed and flowing on the tool rake, and the tool-work interface where the tool flank is rubbing against the newly cut workpiece surface. Therefore, there are theoretically normal load and

friction acting on both the tool rake and the tool flank. It would be difficult to determine the any of the four force components based on a 3-dimensional force measurement by a dynamometer. But if the tool cutting edge is sharp enough, the rubbing and pressing action against the tool flank by the newly cut surface is ignorable. Therefore it will be reasonable to assume that the force components measured on the toolholder are the mere contribution of the resultant normal load $N$, which is perpendicular to the tool rake, and the resultant friction $F$, which is coincident with the resultant chip flow and therefore tangential to the tool rake. For the sake of simplicity, it will also be assumed that the tool-chip contact plane is flat and the obstruction of the attached-on chipbreaker to the chip flowing is ignorable. Then the apparent friction coefficient on the tool chip interface can be defined as the ratio of the frictional force $F$ and the normal load $N$ exerted by the chip on the tool.

Since the cutting force component are usually measured experimentally by a three dimensional dynamometer in the tool-in-use coordinate system [9], i.e. in the directions of cutting, feeding and thrusting for turning operations, resulting in three force components named cutting force $F_{cutting}$, feeding force $F_{feed}$ and thrusting force $F_{thrust}$, respectively, a mechanical model has to be formulated to derive the normal load and frictional forces from these directly measured force components. For an idealized orthogonal cutting, the normal and friction forces can be calculated readily from the cutting force measurements in terms of the rake angle in a two-dimensional hodograph. Yet in industry, most cutting processes are performed in oblique tool configurations, characterized by an inclining angle of the major cutting edge with the cutting velocity. If the inclining angle is small and only the major cutting edge is engaged in the cutting, as in the case of single-edged end-cutting of a thin-walled tubing in a lathe, the conventional two-dimentional hodograph still applies on a plane which contains the directions of the cutting speed and the chip flow. Unfortunately in most turning operations such as the outer diameter

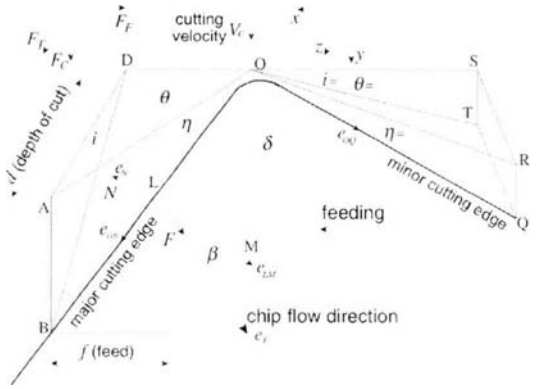


**Fig. 4** Hodograph for general oblique cutting

cutting, the tool nose radius or even a part of the minor cutting edge is usually also engaged in the cutting, causing the chip flow direction to vary with the depth of cut. Therefore, the chip flow angle on the tool rake is not usually equal to the inclination angle, and most toolmakers in practice do not use the effective rake angle to specifiy the tool geometry.

Figure 4 illustrates an oblique cutting model using a conventional tool with a larger nose radius than feed rate. The coordinate axes $x$, $y$, and $z$ are oriented in the directions of the depth of cut (thrusting), cutting and feeding, respectively.

### 2.1 Component projection approach

Since all force components in a three-dimensional oblique cutting is now simplified into a two-dimensional diagram, which is similar to the force diagram for an orthogonal machining, the friction and normal forces can then be easily evaluated. Therefore, all the force components in an oblique cutting model can be projected onto $P$ via the inclination angle $i$. The friction force $F$ can be considered to act on the tool face with a chip flowing angle, which is measured between a perpendicular line to the major cutting edge and the chip edge while the normal force $N$ is defined as perpendicular to the tool rake

All the force components, except the feeding force ($F_{feed}$) and normal force ($N$), have to be rotated for projection. Because the feed force is in the direction of the $z$' axis and the normal

force is in the direction of $y'$ axis, the feed and normal forces are unchanged after projection.

$$F_{feed}'=F_{feed} \tag{1}$$

$$N'=N \tag{2}$$

where the $F_{feed}'$ and $N'$ are the projection of $F_{feed}$ and $N$ on $P$, respectively.

Figure 5 shows the projection of the cutting force, thrusting force, and leads to

$$F_{cutting}'=F_{thrust}\sin i+F_{cutting}\cos i \tag{3}$$

$$F'=F\cos(\eta) \tag{4}$$

where the $F_{cutting}'$ and $F'$ are the projected force on the plane $P$, and $\eta$ is the chip flow angle.

Figure 6 shows all the forces in an oblique cutting process after they are projected to the projection plane $P$ where the following applies

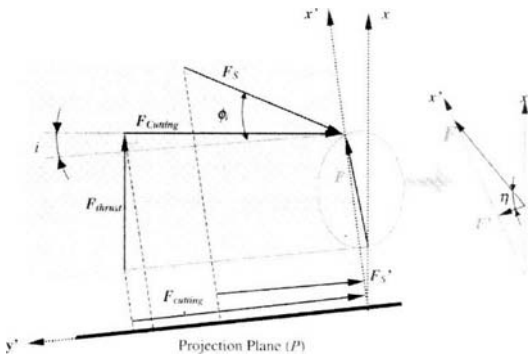


**Fig. 5** The force projection to the plane $P$

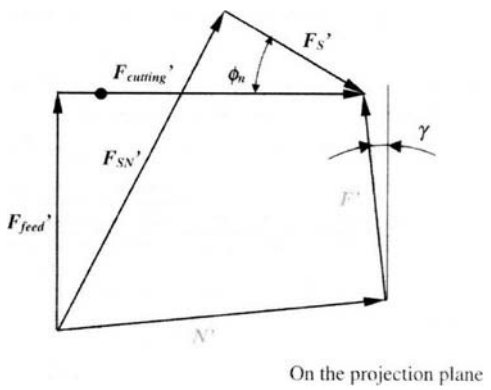


**Fig. 6** The force diagram on the projection plane $P$

$$F'=F_{feed}'\cos\gamma+F_{cutting}'\sin\gamma \tag{5}$$

$$N'=F_{cutting}'\cos\gamma-F_{feed}'\sin\gamma \tag{6}$$

where $\gamma$ is the normal rake angle.

By substituting Equation (1) ~ (4) into Equation (5) and (6), The friction force and normal force can be expressed as

$$F=\frac{F_{feed}\cos\gamma+(F_{cutting}\cos i+F_{thrust}\sin i)\sin\gamma}{\cos\eta} \tag{7}$$

$$N=(F_{cutting}\cos i+F_{thrust}\sin i)\cos\gamma-F_{feed}\sin\gamma \tag{8}$$

### 2.2 Geometric relationship approach

Figure 7 shows the force diagram in a three-dimensional space where the friction and normal forces are resolved into $R_f$, $P_f$ and $R_n$, $P_n$, respectively. $R_f$, and $R_n$ can be evaluated from the cutting and feeding force, while $P_f$ and $P_n$ can be expressed in terms of thrusting and cutting force components. Then the friction force can be written as:

$$F=R_f\cos\eta+F_f\sin\eta \tag{9}$$

Similarly the normal force can be represented as follows:

$$N=R_n\cos i-P_n\sin i \tag{10}$$

The partial components $P_f$ and $P_n$ can be expressed in terms of the cutting force $F_{cutting}$,

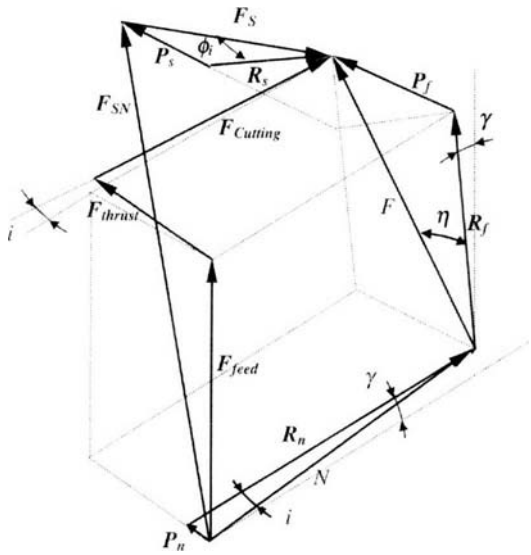


**Fig. 7** The force diagram in oblique cutting model

thrusting force $F_{thrust}$ and inclination angle i as follows

$$P_f = F_{thrust} \cos i + F_{cutting} \sin i \tag{11}$$

$$P_n = -N'' \sin i = -(F_{cutting} \cos i - F_{thrust} \sin i) \sin i \tag{12}$$

where, $N''$ is projection component on plane $x'$-$y'$. $R_f$ and $R_n$ can also be expressed in terms of the feeding force $F_{feed}$, cutting force and the normal rake angle $\gamma$ as

$$R_f = F_{feed} \cos \gamma + F_{cutting} \sin \gamma - P_f \sin i \sin \gamma \tag{13}$$

$$R_n = F_{cutting} \cos \gamma - F_{feed} \sin \gamma - P_f \sin i \cos \gamma \tag{14}$$

In the case of a small rake and inclination angle, the last term in Equation (13) and (14) can be ignored. After $R_f$, $P_f$, $R_n$, $P_n$ in Equation (9) and (10) are substituted by Equation (11)~(14), the friction force and the normal force can be obtained as follows

$$F = (F_{feed} \cos \gamma + F_{cutting} \sin \gamma) \cos \eta + (F_{thrust} \cos i + F_{cutting} \sin i) \sin \eta \tag{15}$$

$$N = (F_{cutting} \cos \gamma - F_{feed} \sin \gamma) \cos i + (F_{cutting} \cos i - F_{thrust} \sin i) \sin^2 i \tag{16}$$

### 2.3 Vector manipulation approach

In this approach, all forces are considered as a vector in $x$-$y$-$z$ coordinate. The direction of the major cutting edge can be represented as a unit vector, $e_{major}$, and a unit vector $e_{minor}$ is also defined along the minor cutting edge. The components of the unit major cutting edge vector $e_{major}$ in $x$-$y$-$z$ coordinate are

$$e_{major} = [\cos i, \ -\sin i, \ 0]^T \tag{17}$$

while the unit minor cutting edge vector $e_{minor}$ is illustrated. Conventionally, tool geometry is specified by an end cutting edge angle $C_e$, rake angle $\gamma$ and oblique angle $I$. Angle $C_e^*$ is the difference between the end edge angle $C_e$ and the side edge angle $C_s$ due to a tool rotation ($C_e^* = C_e - C_s$). Then angle $\lambda$ can be calculated from.

$$\tan \lambda = \frac{\overline{AD}}{\overline{OA}} = -(\tan \gamma + \tan C_e^* \tan i) \cos C_e^* \tag{18}$$

Then the unit minor cutting edge vector can be represented by angle $\lambda$ and $C_e^*$ as follows

$$e_{minor} = [\cos \lambda \sin C_e^*, \ \sin \lambda, \ \cos \lambda \cos C_e^*]^T \tag{19}$$

Thus, the unit normal force vector $e_N$ and the unit friction force vector $e_F$ can be calculated based on the $e_{major}$ and $e_{major}$. The vector, $e_N$, is perpendicular to the rake face. The unit normal vector, $e_N$, to the rake face can be determined as the cross product of these two unit vectors, which are defined by the major and minor cutting edges.

$$e_N = e_{major} \times e_{minor} \tag{20}$$

The frictional force occurs on the rake face in the direction of chip flow. A unit vector $e_F$ can be used to indicate the direction of the friction force. For the sake of convenience, a local coordinate, $e_{major} - e_N - e_{F'}$, can be defined on the rake face to evaluate the unit vector $e_F$ and $e_{F'}$, and the local coordinate $e_{major} - e_N - e_F$ can be calculated by the cross product of $e_N$ and $e_{major}$ because the $e_N$ is already perpendicular to $e_{major}$. Therefore we have

$$e_{F'} = e_N \times e_{major} \tag{21}$$

Thus, the unit frictional force vector in local coordinate $e_{F\,local}$ can be represented by chip flowing angle $\eta$.

$$e_{F\,local} = [\sin \eta, \ 0, \ \cos \eta]^T \tag{22}$$

Obviously, the unit vector $e_F$ in $e_x$-$e_y$-$e_z$ coordinate can be represented from $e_{F\,local}$ in local coordinate by the coordinate transformation. The local coordinate $e_{major} - e_N - e_{F'}$ on the tool face can be denoted by $e_x'$-$e_y'$-$e_z'$ and $e_{major}$, $e_N$, and $e_F'$ is evaluated in $e_x$-$e_y$-$e_z$ coordinate, as

$$\begin{bmatrix} e_x' \\ e_y' \\ e_z' \end{bmatrix} = \begin{bmatrix} e_{major}^T \\ e_N^T \\ e_{F'}^T \end{bmatrix} \begin{bmatrix} e_x \\ e_y \\ e_z \end{bmatrix} \tag{23}$$

and the transformation matrix $[T]$ is

$$[T] = [e_{major}, \ e_N, \ e_{F'}]^T \tag{24}$$

Now obviously, $e_{F\,local}$ can be transformed to $e_F$ by $[T]$.

$$e_{F\,local} = [T] e_F$$

$$e_F = [T]^{-1} e_{F\,local} \tag{25}$$

$$e_F = ([e_{major}, \ e_N, \ e_{F'}])^{-1} e_{F\,local}$$

With the unit vector $e_N$ for the normal force $N$ and $e_F$ for the friction force $F$ ready, the following equations apply

$$N=[F_{thrust},\ -F_{cutting},\ F_{feed}]e_N^T \quad (26)$$

$$F=[F_{thrust},\ -F_{cutting},\ F_{feed}]e_F^T \quad (27)$$

In this research all three types of approaches are introduced, mathematically and theoretically all these methods are coincident, however, as view point of approaching convenience, vector manipulation approaches has more merit to present results.

## 3. Experimental Setup

Cutting tests were performed for both dry and cryogenic cutting of Ti-6Al-4V and AISI1018 on a 30HP (22.4 kW), slant-bed CNC turning center, Cincinnati-Milacron Cinturn 1407C. The CNC controller is programmed to keep the surface cutting speed constant by adjusting the RPM of the spindle automatically with respect to the work diameter. The cutting tool used for both of the materials is an uncoated CNMA432-K68 insert (equivalent to C3 class or ISO05-K20, M10-M20). This rhombic flat insert with a tool holder MCLNL-164C (from Kennametal Inc.) creates a geometrical configuration with the inclining angles of the major cutting edge and the minor cutting edge $i=i'=-5°$, insert nose angle $\delta=80°$, and side angle of the major cutting edge $\theta=95°$. For Ti-6Al-4V, the depth of cut and the feed are selected constantly as 1.27 mm (0.05 inch), 0.254 mm (0.01 inch), respectively, and the surface cutting speeds range from 1.0 m/s, 1.5 m/s, 2.0 m/s to 2.5 m/s. For AISI1018, the depth of cut is changed to 1.52 mm (0.06 inch), while the surface cutting speed elevated to a range from 4 m/s to 11 m/s. To characterize the possible lubrication effect by LN2, different cooling approaches are tested for cutting Ti-6Al-4V, namely, (1) dry cutting (or emulsion cooled cutting), (2) cutting with the primary nozzle shooting LN2 jet to the tool-chip interface (primary nozzle on), (3) cutting with the simultaneous use of the primary and secondary nozzles (2 nozzles on). For all those cutting tests which were performed without activating the primary nozzle (such as in the case of dry cutting, emulsion cooled cutting), the primary nozzle (actually a modified chipbreaker) was still kept in place, but with its LN2 channel blocked, so that the same action of the chipbreaker on the chip flow was in effect for all the cutting tests. The chip flow angle $\eta$ has been measured by a microscope inspection of the wear marking on the tool rake and is listed in Table 3 for each cooling approach.

The compositions of workpieces are described in Table 4. It has good forming and stiffness properties. It is considered to have better machinability than carbon steels with lower carbon content and those with higher carbon content. Typical mechanical properties are shown in Table 4. Those mechanical properties highly depend on the temperature. Keeping cutting area low temperature provides the possibility of improving chip breakability by cryogenic machining. The chip can become brittle and easy to break when the chip temperature is lowered, which results to provide better surface finish.

**Table 3** The chip flow angle (in degrees)

| Ti-6Al-4V | |
|---|---|
| Dry cutting | 8.0 |
| Primary nozzle on | 7.5 |
| Two nozzles on | 7.5 |
| **AISI1018** | |
| Dry cutting | 7.5 |
| Emulsion cooling | 7.0 |
| Primary nozzle on | 7.0 |
| Two nozzles on | 7.0 |

**Table 4** Compositions & mechanical properties

| | Ti-6Al-4V | AISI 1018 |
|---|---|---|
| Tensile Strength (ksi) | 144 | 65 |
| Yield Strength (ksi) | 134 | 48 |
| Elongation (%) | 14 | 36.5 |
| Compositions | 6Al, 4V (%) | 0.15-0.20 C, 0.60-0.90 Mn, 0.04 P, 0.05 S (%) |

## 4. Results and Discussion

The measured cutting force components in titanium machining were converted to the friction force and normal force. Figures 8, 9, and 10 show the friction coefficients versus the cutting speed for cutting Ti-6Al-4V with different cooling conditions. The charts are obtained respectively by the three evaluative approaches. The values of the friction coefficient obtained by each approach match quite well. Obviously, the application of the LN2 to the tool flank together with shooting a LN2 jet to the tool rake (2 nozzles on) can produce an additional lubrication effect to the cutting area, leading to more significant reduction in the friction coefficient, compared to the application of LN2 to the tool rake alone (primary nozzle on). Therefore, the lubrication effect depends considerably on the approaches of the LN2 delivery in cryogenic machining. It can also be seen that the friction coefficient is decrease with cutting speeds as a general trend. The low friction coefficient for these cryogenic cutting tests results mainly from the lubrication, which is made possible by shooting the well-controlled high pressure LN2 jet toward the tool-chip interface. The lubrication effect by LN2 for these cryogenic cutting approaches is due to the greatly changed material properties in the tool-chip contact area, which change a friction mechanism dominated by shearing and galling in the secondary deformation zone of the chip into one that is characterized only by pure sliding. This explains why an additional application of LN2 jet to the tool flank has produced a significant reduction in the friction coefficient at high cutting speeds. On the other hand, the application of LN2 jet to the tool-chip interface may have a tendency of increasing lubrication film by external high pressure between the chip and the tool rake. Therefore, it can be reasonably expected that the generation of a lubrication layer by the LN2 delivery pressure and the change in the material properties at low temperature are combined to reduce the tool-chip friction essentially, with the lubrication effect

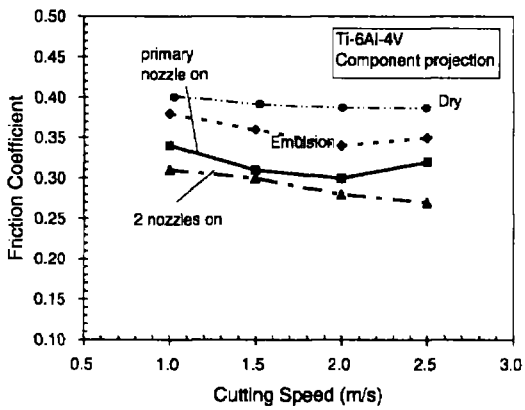


**Fig. 8** Friction coefficient for cutting Ti-6Al-4V (by component projection)

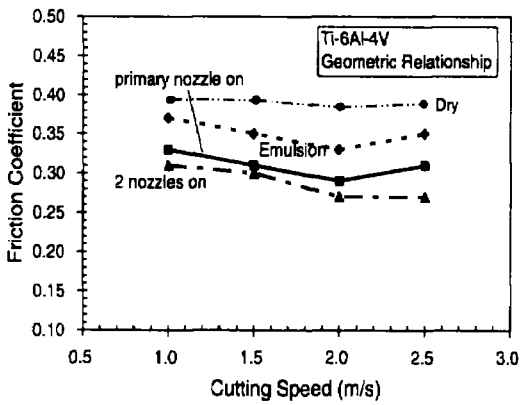


**Fig. 9** Friction coefficient for cutting Ti-6Al-4V (by geometric relationship)

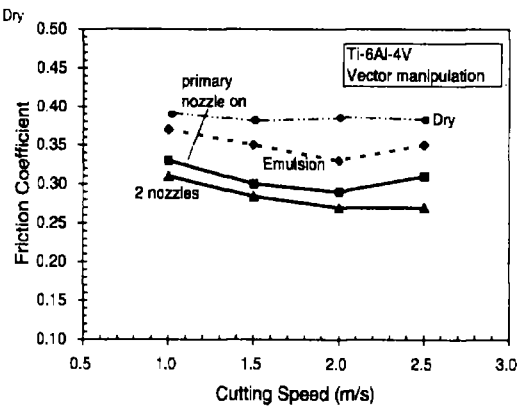


**Fig. 10** Friction coefficient for cutting Ti-6Al-4V (by vector manipulation)

playing the dominating part.

Based on cutting force tests in AISI 1018 machining, the friction coefficient evaluated by the three analytical approaches are presented in Figs. 11, 12, and 13, where the friction coefficient for the emulsion cooled cutting operations is also included for comparison. Compared with the dry or emulsion-cooled cutting, all cryogenic approaches have reduced the friction coefficient considerably at high cutting speeds. Since the hardness and yielding strength for AISI 1018 can be drastically increased with a decreasing temperature, the chip abrasiveness against the tool rake can be considerably enhanced by the low temperature to an extent which overwhelms the positive change in the friction mechanism. This explains why an extra cooling to the tool flank can not necessarily reduce the friction coefficient for cutting AISI1018 at the lower cutting speeds, compared to the mere application of LN2 to the tool-chip interface alone (i.e. primary nozzle on).

The surface roughness value is found to increase substantially with increased feed rate, whereas when the feed rate decreases, the impact of changes in depth of cut on the surface roughness is not as significant in cryogenic machining. Conversely, when the feed rate is increased to 0.32 mm/rev, it can be seen clearly that the surface roughness increases with the increased depth of cut, but the impact of changes in the cutting speed on the surface roughness is less significant. Experimentally with given conditions such as Table 5 the roughness of work-piece is tested with cryogenic cooling and typical cooling and compared as shown Table 6. In cryogenic machining the final roughness is reduced, especially set 3, which conditions cryogenic cooling highly affects roughness is not justifies yet, however, among experimental sets more roughness resulted-case in normal machining is highly reduced in cryogenic machining.

As the temperatures decrease, the brittleness of metal increases usually. Specifically the brittleness of work-pieces is more sensitive than tool material regarding temperatures changes. The more

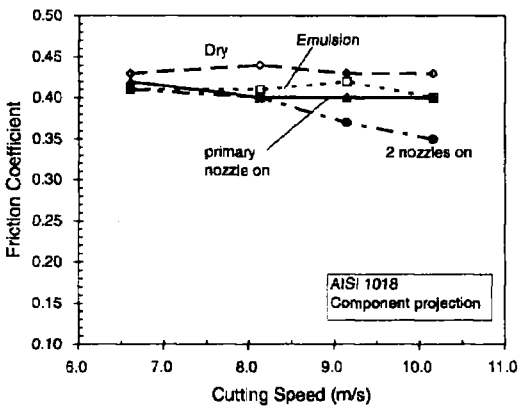


**Fig. 11** Friction coefficient for cutting AISI1018 (by component projection)

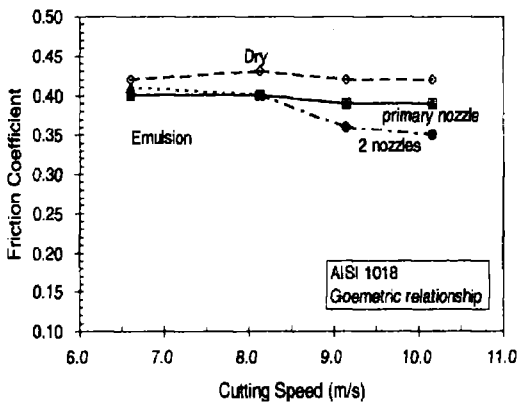


**Fig. 12** Friction coefficient for cutting AISI1018 (by geometric relationship)

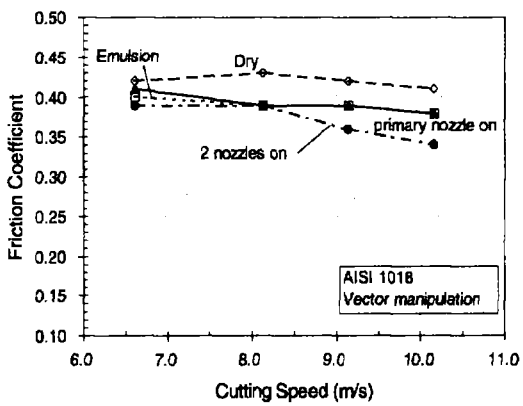


**Fig. 13** Friction coefficient for cutting AISI1018 (by vector manipulation)

brittleness of chip results easier to break it and also produces smoother finishing surface. These result better quality of work-piece finishing in cryogenic machining than conventional machining.

There can be various mechanisms by which the application of LN2 influences the frictional behaviors in cryogenic machining. The application of LN2 tends to reduce the adhesion and chemical reactions between tool rake and chip face, therefore the chip may become less abrasive against the tool face. The substantially reduced tool-chip interface temperature in cryogenic machining can also help in attenuating the degradation of the tool rake, therefore maintaining the surface integrity of the tool rake even at high cutting speed. By using the new LN2 nozzle system, the applied LN2 jet also tends to penetrate into the tool-chip interface, especially with the lifting-up action by the chip breaker, and therefore can generate a lubrication layer by the high delivery pressure of LN2. The partial hydraulic lubrication by the LN2 jets may cause a reduction in the tool-chip contact length, and reduce the resultant frictional force. Due to lower temperature effects on tool and workpiece, the brittleness of properties changes. Therefore, some inter-effects may be issued between tool and workpiece properties. If the brittleness of chip increases, the resulting quality of workpiece is better. Therefore, lower- temperatures-effects on quality issues at tool and workpiece can be resolved.

In all the cutting tests for these two workpiece materials, the friction coefficient tends to decrease with the surface cutting speed. Since the tool-chip interface temperature increases with cutting speed, this tendency can be attributed to the decreased yielding strength of chip, which has lessened the asperity shearing of the chip and tool surface. Therefore, the high speed cryogenic machining can be a good approach to enhancing the lubrication effect of LN2.

**Table 5** Experimental sets

| | Cutting Velocity (m/min) | Feed rate (mm/rev) | Depth of Cut (mm) |
|---|---|---|---|
| Set 1 | 202.63 | 0.2 | 1.25 |
| Set 2 | 121.58 | 0.08 | 0.80 |
| Set 3 | 86.12 | 0.32 | 0.35 |

**Table 6** Roughness of work-piece

| | Normal machining (m) | Cryogenic machining (m) |
|---|---|---|
| Set 1 | 3.111 | 2.345 |
| Set 2 | 3.63 | 3.2 |
| Set 3 | 7.544 | 5.23 |

## 5. Conclusion

To reduce the friction coefficient only optimum amount of injection rate is required, and any extra cooling does not help to reduce the friction. Only ideally designed nozzle is required to decrease the friction, not matter of amount of Nitrogen and number of nozzle. Based on the observation of the frictional behaviors of the tool-chip interface in cryogenic cutting tests, the following conclusion can be drawn

(1) The friction coefficient in cryogenic machining can generally be reduced, depending strongly on the LN2 delivery approach, especially nozzle design and nozzle location.

(2) As long as LN2 is delivered to the tool-chip interface, the friction coefficient can be reduced significantly (approximate 0.3 for Ti-6Al-4V and 0.4 for AISI 1018) and, compared to the dry or emulsion-cooled cutting operations, especially at high cutting speeds. This proves the effectiveness of the hydraulic lubrication of LN2 and underscores the direct exposure of the tool-contact area to the LN2 hydraulics.

(3) The friction coefficient can be reduced to about 0.35 for AISI 1018 and 0.27 for Ti-6Al-4V with two nozzles on.

## Acknowledgment

The authors wish to express their gratitude for the financial support of the cryogenic machining project by the National Science Foundation

(Grant No. DMI-9528710) and the Edison Materials Technology Center (Project No. CT-32), and for the joint partnership with Cincinnati-Milacron, General Motors-Delco Chassis, Timken Company, Kennametal Inc., GE Aircraft Engines, BOC Group, Vortec Co., A.F.Leis Co., Enginetics Co., Abrasive-Form, Inc., and Gem City Engineering.

## References

Arsecularatne, J. A., Fowle, R. F. and Mathew, P., 1998, "Prediction of Chip Flow Direction, Cutting Forces and Surface Roughness in Finish Turning," *J. of Manufacturing Science and Engineering, Transaction of the ASME*, Vol. 120/1, pp.1~7.

Boothroyd, G. and Knight, W. A., 1989, "Fundamentals of Machining and Machine Tools," *Marcel Dekker Inc.*, 2nd edtion.

Fillipi, A. D. and Ippolite, R., 1971, "Facing Milling at −180℃," *Annals* 19 (2), pp. 314~322.

Hong, S. and Ding, Y., 2001, "Cooling Approaches and Cutting Temperatures in Cryogenic Machining of Ti-6Al-4V," *Int. J. of Machine Tools and Manufacture*, Vol. 41/10, pp. 1417~1437.

Hong, S., Markus, I. and Jeong, W., 2001, "New Cooling Approach and Tool Life Improvement in Cryogenic Machining of Titanium Alloy Ti-6Al-4V," *Int. J. of Machine Tools and Manufacture*, Vol. 41/10, pp. 2245~2260

Jainbajranglal, J. R. and Chattopadhyay, A. B, 1984, "Role of Cryogenics in Metal Cutting Industry," *Indian Journal of Cryogenics*, Vol. 0, No. 1, pp. 212~220.

Jawahir, I. S. and Luttervelt, C. A. van, 1993, "Recent Developments in Chip Control Research and Application," *Annals of the CIRP*, Vol. 42, No. 2, pp. 659~693.

Kim, J., Kim, J., Cho, M. and Han, D., 2002, "Friction Characteristics of Piston Ring Pack with Consideration of Mixed Lubrication : Parametric Investigation," *KSME International Journal*, Vol. 16 No. 4, pp. 468~475.

Soo, W. and Kang, P., 2002, "An Investigation on Friction Factors and Heat Transfer Coefficients in a Rectangular Duct with Surface Roughness," *KSME International Journal*, Vol. 16 No. 4, pp. 549~556.

Trend, E. M., 1984, "Metal Cutting," *Butherworths Publication*, London.

Uehara, K. and Kumagai, S., 1969, "Characteristics of Tool Wear in Cryogenic Machining," *J. of Japan Society of Precision Engineers*, Vol. 35, No. 9, pp. 73~77.

Uehara, K. and Kumagai, S., 1998, "Chip Formation, Surface Roughness and Cutting Force in Cryogenic Machining," *Annals of CIRP* 17 (1), pp. 165~172.

Wang, Z. Y and Rujurkar, K. P., 2000, "Cryogenic Machining of Hard-to-cut Materials," *Wear* 239, pp. 168~175.

Wang, Z. Y., Rajurkar, K. P. and Fan J., 1996, "Turning Ti-6Al-4V with Cryogenic Cooling," *Transactions of NAMRI/SME*, Vol. 24, pp. 3~8.